1521-009X/48/12/1303–1311$35.00
DRUG METABOLISM AND DISPOSITION

https://doi.org/10.1124/dmd.120.000098
Drug Metab Dispos 48:1303–1311, December 2020

A Multicompartment Human Kidney Proximal Tubule-on-a-Chip Replicates Cell Polarization–Dependent Cisplatin Toxicity[S]

Tom T.G. Nieskens,[1] Mikael Persson,[1] Edward J. Kelly,[2,3] and Anna-Karin Sjögren[1]

CVRM Safety, Clinical Pharmacology and Safety Sciences, R&D, AstraZeneca, Gothenburg, Sweden (T.T.G.N., M.P., A.-K.S.) and Department of Pharmaceutics and Kidney Research Institute, University of Washington, Seattle, Washington (E.J.K.)

Received April 24, 2020; accepted September 23, 2020

ABSTRACT

Drug-induced kidney injury is a major clinical problem and causes drug attrition in the pharmaceutical industry. To better predict drug-induced kidney injury, kidney in vitro cultures with enhanced physiologic relevance are developed. To mimic the proximal tubule, the main site of adverse drug reactions in the kidney, human-derived renal proximal tubule epithelial cells (HRPTECs) were injected in one of the channels of dual-channel Nortis chips and perfused for 7 days. Tubes of HRPTECs demonstrated expression of tight junction protein 1 (zona occludens-1), lotus lectin, and primary cilia with localization at the apical membrane, indicating an intact proximal tubule brush border. Gene expression of cisplatin efflux transporters multidrug and toxin extrusion transporter (MATE) 1 (*SLC47A1*) and MATE2-k (*SLC47A2*) and megalin endocytosis receptor increased 19.9 ± 5.0–, 23.2 ± 8.4–, and 106 ± 33–fold, respectively, in chip cultures compared with 2-dimensional cultures. Moreover, organic cation transporter 2 (OCT2) (*SLC22A2*) was localized exclusively on the basolateral membrane. When infused from the basolateral compartment, cisplatin (25 μM, 72 hours) induced toxicity, which was evident as reduced cell number and reduced barrier integrity compared with vehicle-treated chip cultures. Coexposure with the OCT2 inhibitor cimetidine (1 mM) abolished cisplatin toxicity. In contrast, infusion of cisplatin from the apical compartment did not induce toxicity, which was in line with polarized localization of cisplatin uptake transport proteins, including OCT2. In conclusion, we developed a dual channel human kidney proximal tubule-on-a-chip with a polarized epithelium, restricting cisplatin sensitivity to the basolateral membrane and suggesting improved physiologic relevance over single-compartment models. Its implementation in drug discovery holds promise to improve future in vitro drug-induced kidney injury studies.

SIGNIFICANCE STATEMENT

Human-derived kidney proximal tubule cells retained characteristics of epithelial polarization in vitro when cultured in the kidney-on-a-chip, and the dual-channel construction allowed for drug exposure using the physiologically relevant compartment. Therefore, cell polarization–dependent cisplatin toxicity could be replicated for the first time in a kidney proximal tubule-on-a-chip. The use of this physiologically relevant model in drug discovery has potential to aid identification of safe novel drugs and contribute to reducing attrition rates due to drug-induced kidney injury.

Introduction

The proximal tubule epithelium is the tissue within the kidney that is most prone to drug-related adverse effects. Renal proximal tubule epithelial cells (RPTECs) are tasked with the active excretion of waste products, including urea and uremic toxins and reabsorption of essential molecules, including water, salts, glucose, amino acids, and proteins (Nigam et al., 2015). To this end, RPTECs express specialized transmembrane drug transporter proteins, facilitating influx from the kidney interstitium and efflux to the glomerular filtrate, which is collectively referred to as transcellular transport, clearing compounds from the internal circulation. Imbalances between influx and efflux, however, can render RPTECs vulnerable to drug-induced toxicity (König et al., 2013; Nigam et al., 2015; Nieskens and Sjögren, 2019).

The main adverse effect of the chemotherapeutic cisplatin is acute kidney injury, which occurs in approximately 30% of patients (Hartmann et al., 1999). Cisplatin is taken up by organic cation transporter 2 (OCT2) (*SLC22A2*), which is located on the basolateral membrane of RPTECs (Ciarimboli et al., 2005; Yonezawa et al., 2005; Filipski et al., 2008; Ciarimboli et al., 2010) and excreted by multidrug and toxin extrusion

This work was supported in part by the AstraZeneca Postdoc Programme.

[1]Current affiliation: CVRM Safety, Clinical Pharmacology and Safety Sciences, AstraZeneca, Gothenburg, Sweden.

[2]Current affiliation: Department of Pharmaceutics, University of Washington, Seattle, Washington.

[3]Current affiliation: Kidney Research Institute, University of Washington, Seattle, Washington.

Primary laboratory of origin: CVRM Safety, Clinical Pharmacology and Safety Sciences, R&D, AstraZeneca, Gothenburg, Sweden.

T.T.G.N., M.P., and A.-K.S. are employees of AstraZeneca AB, Gothenburg, Sweden. T.T.G.N. is a fellow of the AstraZeneca Postdoc Programme.

This work was previously presented as follows in the cited meeting abstract: Nieskens TTG and Sjögren A-K (2019) A functionally polarized human kidney proximal tubule-on-a-chip for advanced drug-induced nephrotoxicity studies. *Winter-meeting in the Danish Society for Pharmacology and Toxicology;* 2019 Dec 02; Copenhagen, Denmark.

https://doi.org/10.1124/dmd.120.000098.

[S]This article has supplemental material available at dmd.aspetjournals.org.

ABBREVIATIONS: 2D, 2-dimensional; 3D, 3-dimensional; DIKI, drug-induced kidney injury; *GAPDH*, glyceraldehyde-3-phosphate dehydrogenase; HBSS, Hanks' balanced salt solution; HRPTEC, human-derived renal proximal tubule epithelial cell; LDH, lactate dehydrogenase; *LRP2*, megalin endocytosis receptor; MATE, multidrug and toxin extrusion transporter; OCT2, organic cation transporter 2.

transporter (MATE) 1 (*SLC47A1*) and to a lesser extent MATE2-k (*SLC47A2*), which is located on the apical membrane of RPTECs (Yonezawa et al., 2006; Nakamura et al., 2010; Li et al., 2013). The toxic potential of cisplatin correlates directly to its accumulation, which is in turn determined by the activity of cation influx and efflux transporters (Li et al., 2013). The physiologic relevance and predictive value of in vitro proximal tubule models for nephrotoxic drugs is therefore in part dependent on the ability to form distinct apical and basolateral membranes, which is referred to as polarization, which enables epithelial barrier formation and correct membrane localization of drug transporters similar to in vivo (Ito et al., 2005; Stoops and Caplan, 2014).

Kidney in vitro models are valuable tools for preclinical investigation of drug-induced toxicity but inherently suffer from partial dedifferentiation (Lash et al., 2006, 2008; Brown et al., 2008). This reduces tight junction expression and epithelial barrier function and limits replication of cell polarization–dependent drug-induced toxicity (Lash et al., 2018). By recapitulating the microenvironment of the physiologic proximal tubule, recently developed kidney-on-a-chip models, which are also known as kidney microphysiologic systems, aim to enhance proximal tubule cultures toward their in vivo phenotype (Jang et al., 2013; Weber et al., 2016; Vedula et al., 2017; Vriend et al., 2018). Epithelial polarization has been confirmed in these chip systems by tight junction formation and the presence of primary cilia (Jang et al., 2013; Jansen et al., 2015; Weber et al., 2016; Vedula et al., 2017; Vormann et al., 2018; Vriend et al., 2018) as well as proof-of-concept studies indicating that transepithelial transport of anionic and cationic organic compounds is feasible (Weber et al., 2016; Jansen et al., 2019; van der Made et al., 2019; Stahl et al., 2020). Kidney-on-a-chip models have been used to study drug-induced toxicity (Jang et al., 2013; Sakolish et al., 2018; Suter-Dick et al., 2018; Weber et al., 2018; Vormann et al., 2018; Maass et al., 2019) but crucially have not previously been applied to study the implications of epithelial polarization and localization of drug transporters for replication of membrane-dependent drug toxicity in vitro.

The aim of this study was to develop a human-derived kidney proximal tubule-on-a-chip that is capable of replicating polarization-dependent nephrotoxicity using cisplatin as model compound. Polarization of the proximal tubule epithelium was demonstrated by apical localization of tight junctions and primary cilia and basolateral localization of OCT2. Moreover, correct polarized localization and function of cisplatin influx transporters were confirmed when toxicity induced by cisplatin was only observed if perfused from the basolateral compartment and not when perfused from the apical compartment. Polarization is crucial for the physiologic relevance of an in vitro model, and when implemented at a fitting stage of drug discovery, this kidney-on-a-chip has the potential to aid the selection of drugs with the right safety profile, improve safety translation, and contribute to bringing safer drugs to the patients.

Materials and Methods

Cell Culture. Cryopreserved human-derived renal proximal tubule epithelial cells (HRPTECs) (batch RPT101030, male, mycoplasma negative) were purchased from Biopredic (Rennes, France). To increase homogeneity, cells of passage 2 were expanded once in T75 Nunc culture flasks (Thermo Fisher, Waltham) before seeding in either 12-well plates or 96-well plates (Corning Life Sciences, Corning, NY) with a density of 75,000 cells/cm^2 for regular monolayer cultures. In the microphysiologic chips (Nortis, Inc., Seattle), cells were seeded at 10×10^6 cells/ml. Cells were incubated at 37°C and 5% v/v CO_2 for 7 days before experimental intervention. Cells were cultured in Dulbecco's modified Eagle's medium/Ham's F12 with GlutaMAX supplement (Life Technologies, Paisley, UK) supplemented with 10 mg/ml insulin, 10 mg/ml transferrin, 10 mg/ml selenium, 24 ng/ml hydrocortisone, 10 ng/ml epidermal growth factor, 4 pg/ml tri-iodothyronine (Sigma, St. Louis), 1% fetal calf serum (Life Technologies), and 1% penicillin/streptomycin (Life Technologies), with the latter used only during seeding. For regular culture plates, the medium was refreshed every 2 to 3 days, whereas medium was continuously perfused in the microphysiologic chips at a rate of 1 μl/min.

Microphysiologic Chip Preparation. Dual-channel microphysiologic chips (dual-channel chip 001), reservoir kits (reservoir kit–001), and all other perfusion equipment was obtained from Nortis, Inc. (Woodinville, WA) and handled according to the manufacturer's instructions. Briefly, the matrix compartment of each chip was first washed with 3 ml ethanol (99.5%; CCS Healthcare, Borlänge, Sweden) and dried by aspiration for 1.5 minutes. Next, rat tail–derived collagen I (7 mg/ml; Corning Life Sciences) was freshly supplemented with Dulbecco's phosphate-buffered saline (1×), phenol red (0.004 mg/ml), HEPES (25 mM), and genipin (0.2 mM); final concentrations are listed. Finally, NaOH and filter-sterilized deionized water were added to obtain a pH of 8.0–8.5. The matrix was subsequently injected into the matrix compartment of each chip and incubated at 4°C for 1 to 2 hours, which was followed by overnight incubation at 37°C for polymerization. The two aligning fiber pins were removed from the chips the next day to form the tubular collagen lumen, with both connecting their respective prefabricated polydimethylsiloxane circuits. The circuits were perfused overnight with culture medium using the Nortis pump setup at 1 μl/min. The next day, only one channel was injected (2×2.5 μl) with freshly prepared collagen IV (10 μg/ml; Sigma) solution in Dulbecco's phosphate-buffered saline (1×), to allow for coating of the lumen and incubated at 37°C and 5% v/v CO_2. After 1 hour, a suspension of cryopreserved HRPTECs in culture medium was injected (2×2.5 μl) into the collagen IV–coated channel at a density of 10×10^6 cells/ml and subsequently incubated at 37°C and 5% v/v CO_2. The matrix ports were closed after 4 hours to prevent drying. Perfusion of both circuits was reinstated after overnight incubation, enabling the remaining unattached cells to flush from the lumen. Medium was continuously perfused through both circuits in the microphysiologic chips at a rate of 1 μl/min (fluid shear stress of 0.9 dyne/cm^2) for 7 days, allowing the cells to form a confluent tube-shaped monolayer.

Compound Exposure, Cell Count, Immunofluorescence Staining, and Barrier Integrity Evaluation. In preparation for compound exposure in microphysiologic chips, medium of the apical channel inflow reservoirs was supplemented with dextran 3000–Alexa Fluor 680 (0.02 mg/ml; Life Technologies). After 1 day, the outflow reservoirs of both the apical channels and basolateral channels were sampled for baseline values. Next, the medium in the apical channel or basolateral channel inflow reservoirs was replaced by medium containing cisplatin (25 μM; Sigma) with or without cimetidine (1 mM; Sigma) depending on the experimental condition. Outflow reservoirs of both channels were sampled at 24, 48, and 72 hours. After 72 hours exposure, nuclear stain was performed by disconnecting chips from the perfusion system and perfused with HBSS (1×, 37°C) supplemented with Hoechst 33342 (1:1000; Life Technologies) at 1 μl/min for 2.5 hours. Benchtop perfusions were performed at room temperature using 5-ml syringes (Henke Sass Wolff, Tuttlingen, Germany) and CMA400 syringe pump (CMA Microdialysis, Kista, Sweden). Chips were imaged immediately at preset excitation and emission wavelengths (Supplemental Table 1) at 20× magnification using ImageXpress Micro Confocal High-Content Imaging System (Molecular Devices, San Jose). The same exposure times were used to establish a baseline in control chips and applied to treatment groups equally. After imaging, chips were treated further for immunofluorescence staining. Counting of nuclei was performed on a single representative section, and single z-slice was focused on the bottom of each tube using "find maxima" in Fiji (version 2.0.0) and a noise tolerance of 600 or 2500 for Hoechst 33342 (depending on the background). Values were expressed as percentage of vehicle, and results were plotted with GraphPad Prism (version 8.01; GraphPad Software). Fluorescence intensity of labeled dextran was evaluated at excitation and emission wavelengths of 670 and 720 nm, respectively, using the Clariostar microplate reader (BMG Labtech, Ortenberg, Germany). Values were expressed as fold change compared with baseline, and results were plotted with GraphPad Prism (version 8.01; GraphPad Software).

For immunofluorescence staining, chips were disconnected from the perfusion system and first perfused with HBSS (1×, 37°C) at 1 μl/min for 2.5 hours. Next, chips were perfused with formaldehyde (4%; VWR, Spånga, Sweden) at 1 μl/min for 1.5 hours, which was followed by wash buffer at 10 μl/min for 1 hour. Wash buffer consisted of bovine serum albumin (2%; Sigma) and Triton × 100 (1%; Sigma) in HBSS. Primary antibody was diluted to the indicated ratio in wash buffer (Supplemental Table 1) and subsequently manually injected (200 μl) into the chips, which was followed by overnight incubation at 4°C. Next day, chips

were first perfused with wash buffer at 10 μl/min for 1 hour, which was followed by manual injection (200 μl) of secondary antibody (Supplemental Table 1) supplemented with Hoechst 33342 (1:1000; Life Technologies) and optionally phalloidin–Alexa Fluor 647 (1:100; Life Technologies). The chips were perfused with wash buffer at 10 μl/min for 1 hour before imaging at preset excitation and emission wavelengths (Supplemental Table 1) at 20× magnification using ImageXpress Micro Confocal High-Content Imaging System (Molecular Devices). The intensity profile of the images was automatically rescaled to correct for background for visualization only, and image montages were made using Fiji (version 2.0.0). For 3-dimensional (3D) reconstruction of tight junctions, the spinning disk confocal function (60-μm pinhole) was enabled before images were taken every 2 μm over 120 μm in the z-direction. Reconstruction was performed using "3D Project" in Fiji with "brightest point method," 2-μm spacing between images, and turning the resulting tube to an angle of 30°.

Gene Expression Analysis. For gene expression analysis in microphysiologic chips, chips were disconnected from the perfusion system and first perfused with HBSS (1×, 37°C) at 1 μl/min for 2.5 hours. Next, chips were perfused with RLT lysis buffer (Qiagen, Hilden, Germany) at 5 μl/min for 30 minutes, and the perfusate was collected. After a static incubation for 30 minutes, chips were perfused again with RLT lysis buffer (Qiagen) at 5 μl/min for 40 minutes, thus collecting the perfusate. For gene expression analysis in regular monolayer cultures, cells seeded in 12-well plates were first washed 3× with HBSS (1×) and directly lysed in RLT lysis buffer (0.5 ml/well; Qiagen). RNA was isolated using the RNeasy Mini kit (Qiagen) according to the instructions as provided by the manufacturer. High Capacity cDNA Reverse Transcription kit (Applied Biosystems, Foster City) was used to synthesize cDNA at a final concentration of 6 ng/μl according to the instructions as provided by the manufacturer. Expression levels of mRNA were determined using gene-specific primer probe sets (Supplemental Table 2) and Taqman Fast Advanced Master Mix (Applied Biosystems) using the QuantStudio Flex 7 (Applied Biosystems) at a final concentration of 1.8 ng/μl cDNA and analyzed using Quantstudio Real Time PCR Software (version 1.3; Applied Biosystems). Expression levels in the microphysiologic chips were expressed as $-\Delta\Delta C_t$ compared with regular monolayer cultures using *GAPDH* as reference gene. Results were plotted with GraphPad Prism (version 8.01; GraphPad Software).

Transcellular 4-Di-1-ASP Transport Assay. To evaluate transcellular transport capability of cations in microphysiologic chips, chips were disconnected from the perfusion system and first perfused with HBSS (1×, 37°C) supplemented with HEPES (10 mM; Life Technologies) at 1 μl/min for 3 hours. Next, perfusion of the basolateral channel was switched to HBSS-HEPES containing 4-di-1-ASP (100 μM; Life Technologies) with or without cimetidine (1 mM; Sigma) at 2 μl/min. The apical channel was perfused with HBSS-HEPES. Accumulative perfusate samples were collected from 6 hours after initiation of perfusion for 14 hours. Finally, 100 μl of each sample was transferred to a 96-well plate and fluorescence intensity of 4-di-1-ASP was evaluated at excitation and emission wavelengths of 485 and 590 nm, respectively, and a gain of 1600 using the Clariostar microplate reader (BMG Labtech). Values were expressed as arbitrary units or blank-subtracted and normalized against uninhibited control. Results were plotted with GraphPad Prism (version 8.01; GraphPad Software).

Lactate Dehydrogenase Evaluation. Lactate dehydrogenase (LDH), as measure for cell-membrane integrity in regular 2-dimensional (2D) cultures, was evaluated from supernatant (10 μl) using the Pierce LDH Cytotoxicity Assay Kit (Thermo Fisher) according to the instructions as provided by the manufacturer. Reactions were run for 30 minutes, and absorbance was evaluated at 490 and 680 nm using the Clariostar microplate reader (BMG Labtech). Values at 680 mn were subtracted from 490 nm, and results were plotted with GraphPad Prism (version 8.01; GraphPad Software).

Cisplatin Exposure Measurements. To estimate the concentration chip-cultured cells are exposed to when cisplatin is perfused from the basolateral and apical compartments, chips were prepared as described earlier while cell injection was omitted to eliminate any drug-transporter or metabolic-related effects. Basolateral exposure was evaluated by perfusing one channel with cisplatin (25 μM; Sigma) and the other with medium and collecting perfusate from the medium channels. Apical exposure was evaluated by perfusing only one channel with cisplatin (25 μM; Sigma) and collecting from the same, whereas the parallel channel was not perfused. Perfusions were performed using the Nortis pump setup at 1 μl/min, and samples were taken every 12 hours for 72 hours. Samples were processed first by passing them through a Microcon 30-kDa microcentrifuge filter unit (Ultracel-30 membrane; Merck-Millipore, Burlington, MA) using centrifugation for 10 minutes at 16,000*g* and 4°C, filtrate (20 μl), diluted with internal standard, and derivatized with diethylthiocarbamate (5% diethyldithiocarbamate in sodium hydroxide solution; Sigma). Samples were diluted with acetonitrile/water (1/1 v/v), and cisplatin content was evaluated by high-pressure liquid chromatography coupled to tandem mass spectrometry. Separation of derivatized cisplatin was achieved using high-pressure liquid chromatography with an Acquity BEH C18 column (Waters, Milford, MA) and acetonitrile/acetic acid (100/0.2 v/v) and ammonium formate (20 mM) mobile phase run under gradient conditions. Detection was via an API5000 mass spectrometer (Sciex, Framingham, MA) in positive TurboIonSpray mode, and results were plotted with GraphPad Prism (version 8.01; GraphPad Software).

Statistical Analysis. All data analysis and statistics were performed using GraphPad Prism (version 8.01; GraphPad Software) and presented as mean ± S.D. of three independent experiments ($n = 3$) set in advance unless stated otherwise. The number of experimental replicates and total comparisons is indicated in the figure legends. Statistics were performed by (paired) Student's *t* tests (two-tailed, a = 0.05) and corrected for multiple comparisons using the Holm-Sidak method and one- or two-way ANOVA with Dunnett's multiple comparisons test ($P < 0.05$) using multiplicity-adjusted *P* values.

Results

HRPTECs Cultured in the Kidney Proximal Tubule-on-a-Chip Were Polarized with Tight Junctions, and Primary Cilia Localized on the Apical Brush Border and OCT2 Were Strictly Localized on the Basolateral Membrane. To increase the physiologic relevance of the culture environment, HRPTECs were cultured in Nortis dual-channel microphysiologic chips. These consist of two parallel collagen IV–coated hollow channels inside a larger compound-permeable collagen I matrix that allows for independent medium perfusion through separate channel circuits (Fig. 1A). When HRPTECs were injected into a single channel and perfused with culture medium at 1 μl/min (fluid shear stress of 0.9 dyne/cm^2), cells attached directly to collagen IV, and 3D tube formation was observed over the course of 7 days (Fig. 1B). The remaining empty channel was also perfused, generating a culture system with distinct apical and basolateral compartments, thus representing the tubule lumen and the kidney interstitium, respectively. To investigate cellular polarization, HRPTECs were subsequently stained with antibodies for confocal fluorescence imaging at the positions indicated in Fig. 1E. Tubes demonstrated a characteristic epithelial expression pattern of tight junction protein highlighting cell-cell interactions with focused expression at the apical membrane (Fig. 1C). A 3D reconstruction of the tight junction pattern using confocal imaging confirmed an elongated, tube-shaped tissue structure (Fig. 1D). In addition, tubes showed apical localization of lotus lectin, the presence of primary cilia protruding from the apical membrane into the tubule lumen (by staining for acetylated α tubulin), and strict basolateral localization of OCT2 (Fig. 1C), which together demonstrated an intact tubule brush border that is tight and polarized. Finally, phalloidin was used to demonstrate that F-actin is mainly located at the cell borders and the basolateral membrane, which is a typical distribution for epithelial cells (Fig. 1C).

Gene Expression of MATE1 and MATE2-k Efflux Drug Transporters Increased in HRPTECs Cultured in the Kidney Proximal Tubule-on-a-Chip Compared with Regular 2D Cultures. Next, gene expression of several drug transporters and proximal tubule markers in chip-cultured HRPTECs was compared with regular 2D HRPTEC cultures (Fig. 2; Table 1). Expression of MATE1 (*SLC47A1*) and MATE2-k (*SLC47A2*), which are both responsible for cisplatin efflux, increased 19.9 ± 5.0– and 23.2 ± 8.4–fold (mean ± S.D., $n = 5$), respectively, when HRTPECs were cultured in the chips as compared with regular 2D cultures (Fig. 2; Table 1). Cisplatin-uptake transporters OCT2 (*SLC22A2*) and high-affinity copper-uptake transporter 1 (*SLC31A1*)

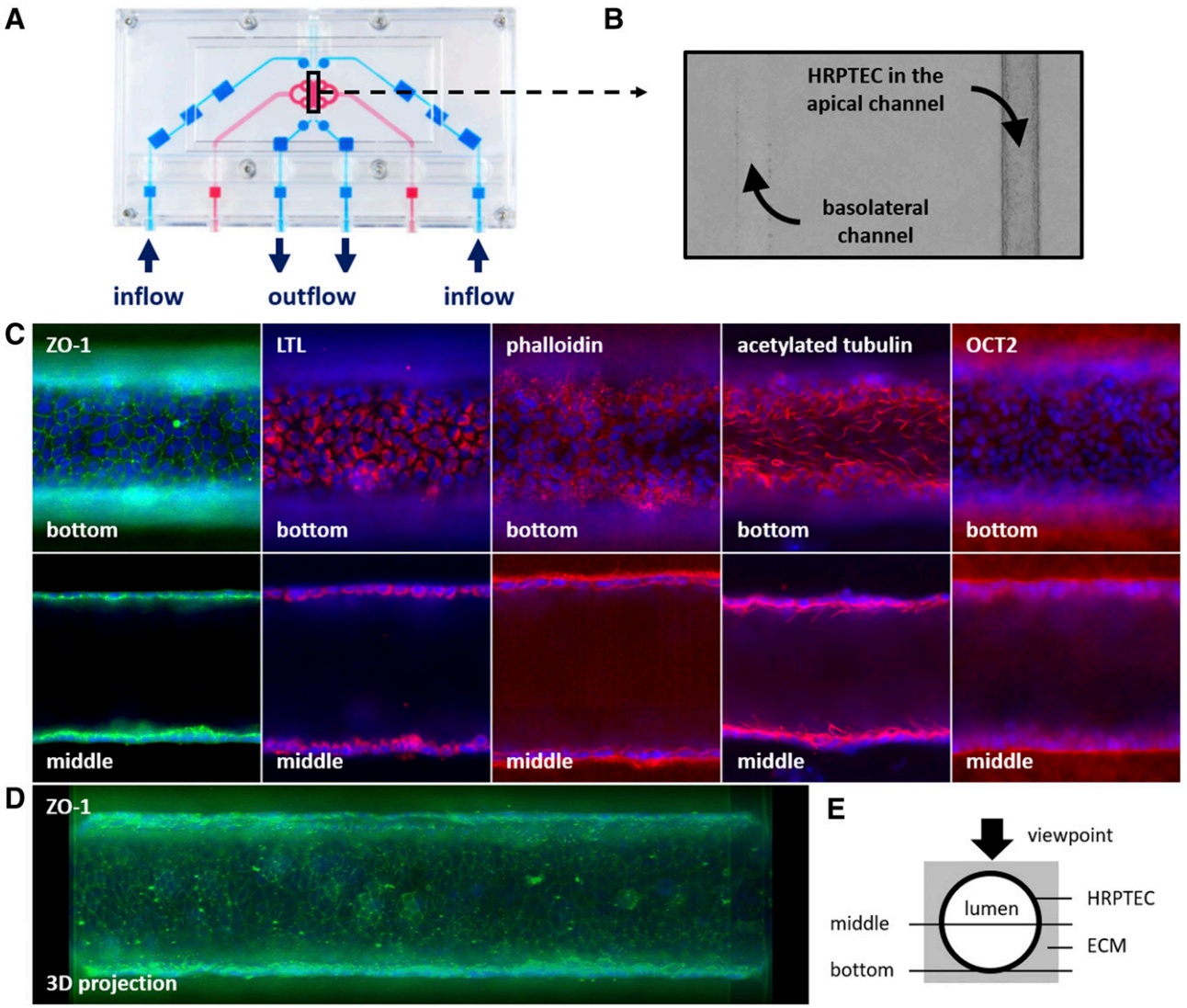

Fig. 1. Characterization of the polarized human-derived kidney proximal tubule-on-a-chip. (A) Layout of the Nortis dual-channel chip with the extracellular matrix compartment (ECM, red), which contains two hollow channels (black box) that are coupled to an independent polydimethylsiloxane perfusion circuit (blue), which are in turn fed by medium reservoirs located at the inflow positions. Courtesy of Nortis, Inc. (B) Phase contrast image shows that a 3D HRPTECs tube is formed inside the hollow channel after injection and medium perfusion for 7 days with a distinct luminal compartment forming the apical channel, whereas the parallel basolateral channel is only perfused with medium (original magnification, 4×). (C) Immunofluorescent confocal image shows a typical epithelial localization pattern of tight junction protein (zona occludens-1, *TJP1*) at the interface between HRPTECs and positive staining for HRPTECs marker lotus lectin (LTL); both are correctly localized at the apical brush border membrane on the luminal side of the tube. Phalloidin stained for F-actin that outlines the borders of HRPTECs, and OCT2 (*SLC22A2*) is strictly localized on the basolateral membrane on the ECM side of the tube. Staining for acetylated α tubulin demonstrates the presence of primary cilia protruding from the apical membrane into the tubule lumen, thus confirming epithelial polarization of HRPTECs in the proximal tubule-on-a-chip. (D) 3D projection (30°) of 60 confocal microscopy planes demonstrates the continuity of tight junction protein [zona occludens-1 (ZO-1)] immunofluorescent staining throughout the HRPTECs tube. (E) Cut-through overview of the proximal tubule-on-a-chip and imaging positions used for confocal microscopy.

were expressed at similar levels in chip-cultured and regular 2D-cultured HRPTECs (Fig. 2; Table 1). In addition, chip-cultured HRPTECs increased expression of megalin endocytosis receptor (*LRP2*) with 106 ± 33–fold (mean ± S.D., $n = 5$) and expression of efflux transporter breast cancer resistance protein (*ABCG2*) with 4.3 ± 0.4–fold (mean ± S.D., $n = 3$), whereas the expression of efflux transporter P-glycoprotein (*ABCB1*) was decreased to 0.32 ± 0.06–fold (mean ± S.D., $n = 5$) (Fig. 2; Table 1). Interestingly, organic anion transporter 1 (*SLC22A6*) was expressed exclusively in chip-cultured HRPTECs (ΔC_t of 11.8 ± 0.8 relative to *GAPDH*, $n = 5$, Table 1) and was not detected in regular 2D cultures. Gene expression of organic anion transporter 3 (*SLC22A8*) was, however, not detected in either regular 2D or chip-cultured HRPTECs (Table 1).

A Trend toward Transepithelial Transport of Fluorescent Organic Cation 4-Di-1-ASP Was Observed in the Kidney Proximal Tubule-on-a-Chip. To investigate the concerted activity of cation influx and efflux transport mechanisms in the human kidney proximal tubule-on-a-chip, transcellular transport of 4-di-1-ASP was evaluated. The fluorescent organic cation 4-di-1-ASP is reported to be a substrate for both OCT2 and MATE1/2-k drug transporters covering the cation transcellular transport axis (Biermann et al., 2006; Wittwer et al., 2013). To this end, 4-di-1-ASP (100 μM) was perfused into the basolateral compartment while buffer was perfused into the apical compartment so that fluorescence intensity of accumulative apical perfusate (14 hours) reflected compound transfer (Fig. 3A). As expected, the apical fluorescence signal was reduced compared with the

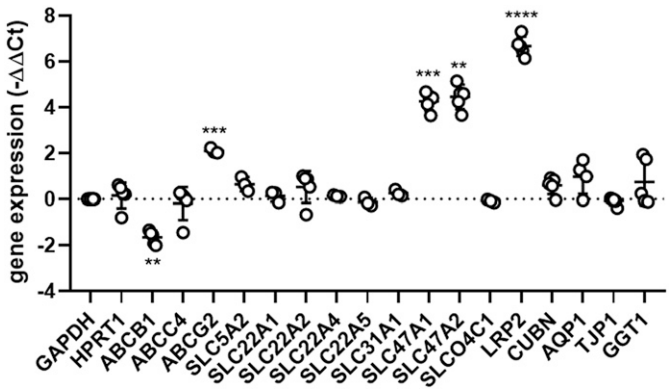

Fig. 2. Gene expression levels in human-derived kidney proximal tubule cells cultured in the chip compared with regular 2D cultures. Gene expression analysis of drug transporters, endocytosis receptors, and proximal tubule epithelial cell markers show significantly higher MATE1 (*SLC47A1*), MATE2-k (*SLC47A2*), breast cancer resistance protein (*ABCG2*), and *LRP2* gene expression in HRPTECs cultured for 7 days in chips compared with HRPTECs cultured for the same time in 2D, whereas expression of P-glycoprotein (*ABCB1*) is reduced when using *GAPDH* as reference gene [mean ± S.D., gene expression in chip-cultured HRPTECs compared with 2D cultures by multiple Student's *t* tests $n = 5$ (number of biologic replicates set in advance except when otherwise indicated); $n = 8$ (*GAPDH*; due to inclusion of additional biologic replicates after experimental design); $n = 4$ (*AQP1*; due to technical error); and $n = 3$ (*ABCG2, SLC5A2, SLC22A1, SLC22A4, SLC22A5, SLC31A1, SLCO4C1*; due to inclusion after experimental design) performed with one experimental replicate with 18 comparisons in total, and $^{**}P < 0.01$, $^{***}P < 0.001$, and $^{****}P < 0.0001$ (corrected for multiple comparisons using the Holm-Sidak method)]. *AQP1*, aquaporin 1; *CUBN*, cubilin; *GGT1*,gamma-glutamyltransferase 1; *HPRT1*, hypoxanthine phosphoribosyltransferase 1; *TJP1*, tight junction protein 1.

basolateral signal because it reflects HRPTEC epithelial barrier integrity (Supplemental Fig. 1). The active transport component was evaluated by supplementing 4-di-1-ASP with competitive OCT2 inhibitor cimetidine (1 mM, Fig. 3B). A trend toward cimetidine-mediated inhibition of 4-di-1-ASP transfer was observed in every individual experiment [66%, 30%, and 17%; with an average of 38% ± 25% (mean ± S.D., $n = 3$, Fig. 3B)] but was not statistically significant (paired Student's *t* test, $P = 0.18$).

Cisplatin-Induced Toxicity in the Kidney Proximal Tubule-on-a-Chip Exclusively when Exposed to the Basolateral Membrane, and Toxicity Was Abolished by the OCT2 Inhibitor Cimetidine. When HRPTECs were cultured in regular 96-well plates, cisplatin (12.5–50 μM) induced toxicity, as demonstrated by a time- and concentration-dependent increase of LDH in the supernatant (Supplemental Fig. 2). As expected, toxicity was attenuated by coincubation with cimetidine (1 mM), indicating its dependence on OCT2 influx activity (Supplemental Fig. 2). In contrast to regular 2D cultures, the dual-channel chip layout allows for selective exposure of the proximal tubule apical or basolateral membrane, which is relevant when mimicking physiologic exposure to therapeutics in vitro. When cisplatin (25 μM) was perfused for 72 hours from the basolateral channel, mimicking exposure through the clinically relevant interstitium and internal circulation, the tight junction pattern on the bottom slice of the tube was partly disrupted (Fig. 4A), and cell count was reduced to 41.2% ± 6.6% (mean ± S.D., $n = 5$) compared with vehicle control (Fig. 4B). This resulted in a concomitant 8.7 ± 6.3–fold (mean ± S.D., $n = 4$) increase in paracellular diffusion of dextran 3000 across the epithelium from the apical compartment into the basolateral compartment (Fig. 4C). As expected, coincubation with the OCT2 inhibitor cimetidine (1 mM) abolished all toxic effects, demonstrating that cisplatin-induced toxicity is dependent on OCT2 influx activity (Fig. 4, A–C). The actual concentration of cisplatin reaching the cells through basolateral exposure was measured by omitting cell injections, perfusing the basolateral channel with cisplatin (25 μM), and collecting the perfusate from the apical channel (Fig. 5A). The resulting concentration of cisplatin was 3.4 ± 0.05 μM (at 24 hours, mean ± S.D., $n = 3$, Fig. 5C), which is similar to clinical therapeutic total plasma concentrations reported in literature, although this is dependent on the dosing regimen applied (Himmelstein et al., 1981; Ikeda et al., 1998; Petrillo et al., 2019). In contrast, when cisplatin was perfused from the apical channel mimicking exposure through the tubule lumen,

TABLE 1

Gene expression levels of drug transporters, endocytosis receptors, tight junction protein, and proximal tubule markers in regular 2D cultures and Nortis chip cultures of HRPTECs[a]

Gene	Ct		−ΔΔCt	
	2D HRPTECs	Nortis HRPTECs	2D HRPTECs	Nortis HRPTECs
GAPDH	16.2 ± 1.1	17.4 ± 0.5		
HPRT1	20.9 ± 0.9	22.2 ± 0.5	0.0 ± 0.4	0.2 ± 0.6
ABCB1	19.9 ± 0.8	23.0 ± 0.4	0.0 ± 0.6	−1.7 ± 0.3
ABCC4	21.5 ± 0.9	23.1 ± 0.7	0.0 ± 0.4	−0.2 ± 0.7
ABCG2	34.5 ± 0.2	33.0 ± 0.4	0.0 ± 0.1	2.1 ± 0.1
SLC5A2	32.4 ± 0.2	32.3 ± 0.2	0.0 ± 0.3	0.6 ± 0.3
SLC22A1	31.4 ± 0.1	31.9 ± 0.3	0.0 ± 0.2	0.1 ± 0.2
SLC22A2	24.2 ± 0.5	25.1 ± 0.6	0.0 ± 0.9	0.5 ± 0.7
SLC22A4	28.5 ± 0.1	28.9 ± 0.4	0.0 ± 0.1	0.1 ± 0.1
SLC22A5	25.6 ± 0.1	26.4 ± 0.2	0.0 ± 0.1	−0.1 ± 0.1
SLC22A6	N.D[b]	29.0 ± 0.8		
SLC22A8	N.D[b]	N.D[b]		
SLC31A1	24.2 ± 0.1	24.6 ± 0.2	0.0 ± 0.1	0.3 ± 0.1
SLC47A1	31.0 ± 0.4	28.2 ± 0.4	0.0 ± 1.0	4.3 ± 0.4
SLC47A2	28.7 ± 1.5	25.7 ± 0.4	0.0 ± 1.8	4.5 ± 0.5
SLCO4C1	22.2 ± 0.1	22.9 ± 0.3	0.0 ± 0.1	−0.1 ± 0.1
LRP2	34.0 ± 1.8	28.7 ± 0.5	0.0 ± 1.4	6.7 ± 0.4
CUBN	27.1 ± 0.7	27.9 ± 0.4	0.0 ± 0.5	0.6 ± 0.4
AQP1	23.1 ± 0.8	23.2 ± 0.7	0.0 ± 0.6	1.0 ± 0.7
TJP1	20.7 ± 0.9	21.8 ± 0.5	0.0 ± 0.3	−0.1 ± 0.2
GGT1	19.6 ± 1.8	19.7 ± 1.5	0.0 ± 1.1	0.7 ± 1.0

AQP1, aquaporin 1; *CUBN*, cubilin; *GGT1*,gamma-glutamyltransferase 1; *HPRT1*, hypoxanthine phosphoribosyltransferase 1; *TJP1*, tight junction protein 1.
[a]Mean ± S.D.
[b]Not detected.

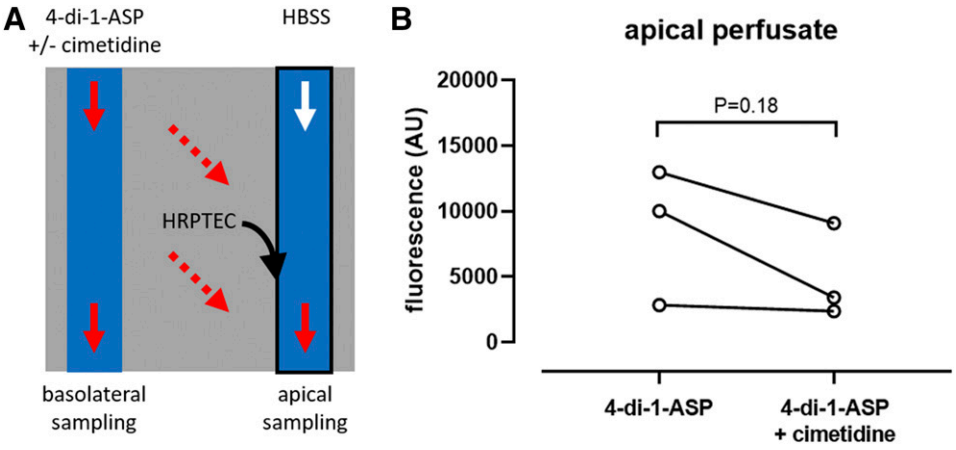

Fig. 3. Transepithelial transfer of fluorescent organic cation 4-di-1-ASP in the proximal tubule-on-a-chip. (A) Fluorescent cation 4-di-1-ASP (100 μM) was perfused at 2 μl/min into the basolateral compartment of the proximal tubule-on-a-chip with or without competitive OCT2 inhibitor cimetidine (1 mM), whereas HBSS-HEPES buffer was perfused into the apical compartment. (B) Fluorescence intensity of 4-di-1-ASP in accumulative apical perfusate (8612 ± 5208) was not significantly reduced (P = 0.18) upon coincubation with cimetidine (1 mM) [4956 ± 3616, mean ± S.D., fluorescence intensity of the apical perfusate without cimetidine compared with cimetidine by paired Student's t test, n = 3 (with the number of biologic replicates set in advance), performed with one experimental replicate, one comparison in total].

toxicity was not observed (Fig. 4, A–C). The concentration of cisplatin through apical exposure was evaluated by perfusing the apical channel with cisplatin (25 μM) and collecting perfusate from the apical channel (Fig. 5B), resulting in an actual exposure of 20.2 ± 1.3 μM (at 24 hours, mean ± S.D., n = 3, Fig. 5C). So, even though apical cisplatin exposure was more than 5-fold higher than the basolateral exposure, it did not induce toxicity. These results confirm that the transporters meditating cisplatin toxicity were uniquely expressed on the basolateral membrane, supporting the epithelial polarization of this proximal tubule-on-a-chip.

Discussion

Achieving a safety profile for candidate drugs lacking renal adverse effects prior to the clinical phase of development requires predictive and physiologically relevant in vitro proximal tubule epithelial models.

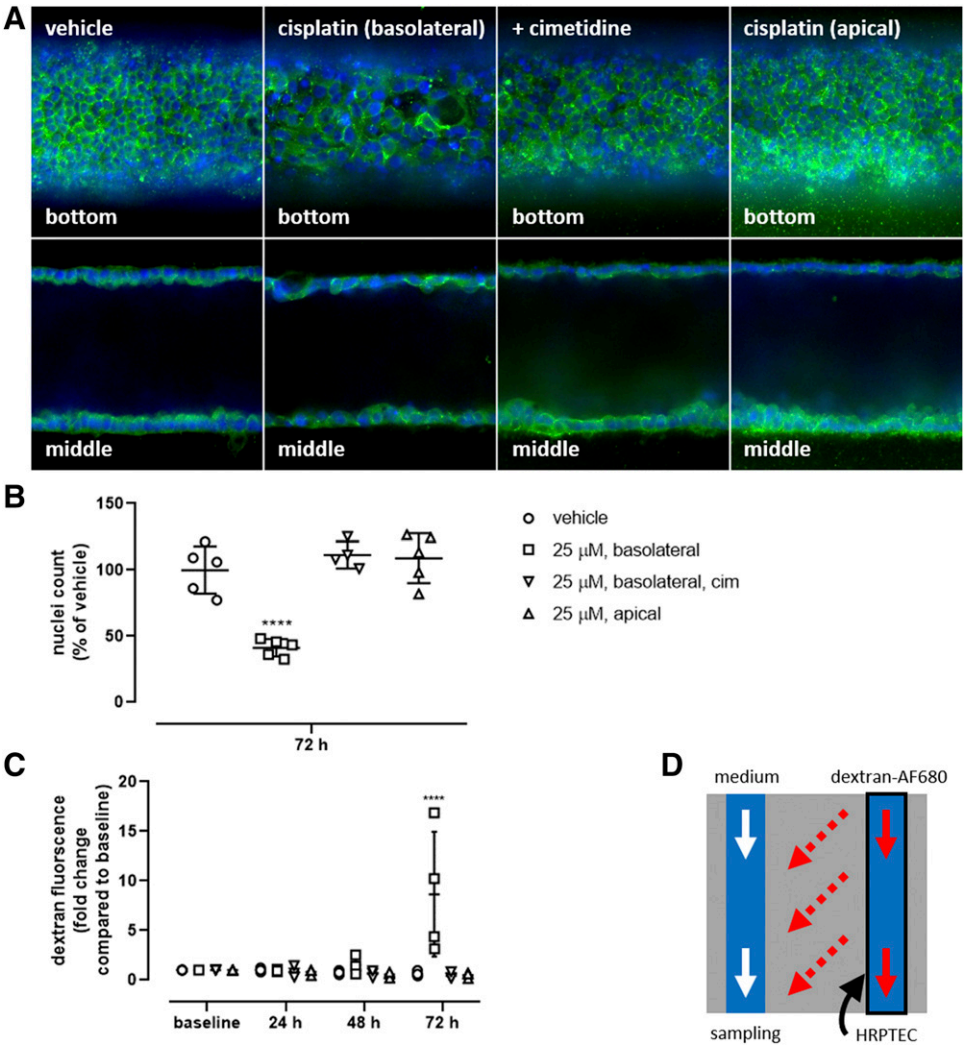

Fig. 4. Membrane-dependent cisplatin-induced toxicity in the human-derived kidney proximal tubule-on-a-chip. Cisplatin (25 μM, 72 hours) induced toxicity when perfused from the basolateral compartment but not the apical compartment and is abolished by coperfusion with OCT2 inhibitor cimetidine (1 mM) as evaluated by (A) disruption of tight junctions at the bottom and middle planes of chip-cultured HRPTECs, (B) reduced nuclei count, and (C) reduced epithelial barrier integrity according to the figure in (D). Analysis of (A) [n = 5 (vehicle; 25 μM basolateral; 25 μM apical) and n = 4 (25 μM basolateral, cimetidine) with all biologic replicates set in advance, performed with one experimental replicate, and representative images were selected, original magnification, 20×]. (B) Mean ± S.D., Hoechst count in the "bottom" images compared with vehicle by one-way ANOVA with Dunnett's multiple comparisons test, n = 5 (vehicle; 25 μM basolateral; 25 μM apical) and n = 4 (25 μM basolateral, cimetidine) with all biologic replicates set in advance, performed with one experimental replicate, with three comparisons in total; ****$P < 0.0001$ (multiplicity-adjusted P values). (C) Mean ± S.D., dextran 3000–Alexa Fluor 680 fluorescence intensity sampled from the basolateral channel perfusate compared with time-matched vehicle by two-way ANOVA with Dunnett's multiple comparisons test, n = 4 (vehicle; 25 μM basolateral; 25 μM apical) and n = 3 (25 μM basolateral, cimetidine) with one biologic replicate excluded because of technical error, performed with one experimental replicate, with 12 comparisons in total; ****$P < 0.0001$ (multiplicity-adjusted P values). Cim, supplemented with cimetidine (1 mM).

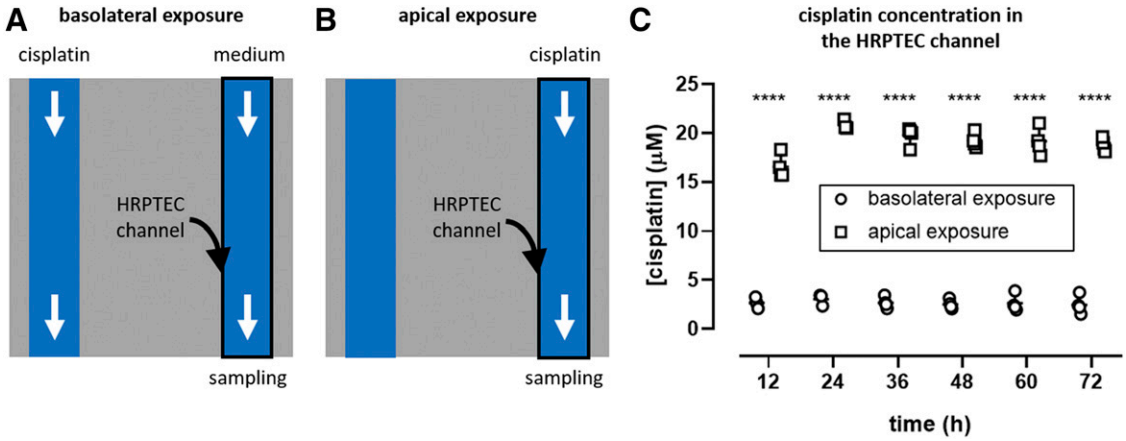

Fig. 5. Differences in exposure of the HPRTEC channel depending on basolateral or apical perfusion of cisplatin. (A) Basolateral perfusion aims to mimic clinically relevant exposure by perfusing cisplatin into the basolateral (parallel) channel followed by diffusion through the collagen I matrix, resulting in exclusive exposure of the HRPTEC basolateral membrane. (B) Apical perfusion of cisplatin directly in the apical HRPTEC channel. (C) Cisplatin concentration in the HRPTEC channel is significantly reduced when cisplatin (25 μM) is perfused through the basolateral compartment compared with the apical compartment as indicated in (A and B) taking nonaccumulating samples every 12 hours for 72 hours [mean ± S.D., basolateral concentration compared with time-matched apical concentration by multiple Student's *t* tests; $n = 4$ (12, 36–72 hours) and $n = 3$ (24 hour) with one biologic replicate at 24 hour excluded because of technical error, performed with one experimental replicate, six comparisons in total; ****$P < 0.0001$ (corrected for multiple comparisons using the Holm-Sidak method)].

Here, we developed a human-derived kidney proximal tubule-on-a-chip that demonstrates epithelial polarization with intact tight junctions and primary cilia on the apical brush border membrane and strict localization of OCT2 on the basolateral membrane. Exclusive OCT2-dependent sensitivity to the nephrotoxic drug cisplatin was shown when the tube was exposed via the basolateral compartment, whereas toxicity was not observed when exposed to more than 5-fold higher concentration via the apical compartment. Therefore, the importance of polarized localization of cation drug uptake transporters to more accurately replicate drug-induced kidney toxicity was demonstrated for the first time in a chip-based proximal tubule model.

Influx of cisplatin into renal proximal tubule epithelial cells and the nephrotoxicity this results in have been shown to be mediated by OCT2 (Ciarimboli et al., 2005, 2010; Yonezawa et al., 2005, 2006) and high-affinity copper-uptake protein 1 (*SLC31A1*) (Pabla et al., 2009). OCT2 is a facilitated diffusion transporter driving the influx of cationic compounds across the basolateral membrane using the inward-directed negative membrane potential (Okuda et al., 1999b; Budiman et al., 2000). The current study showed attenuation of cisplatin toxicity by cimetidine in both regular 2D HRPTEC cultures and chip-cultured HRPTECs, demonstrating OCT2 activity is the main contributing factor to cisplatin toxicity and confirming previous results in vitro (Yonezawa et al., 2005, 2006; Sato et al., 2008) and in vivo (Ciarimboli et al., 2010; Katsuda et al., 2010). It is worth noticing, however, that the cimetidine concentration used is higher than a typical pharmacological concentration, as the C_{max} is reported to be 16 μM (Schmidt et al., 1998). Moreover, the current study elegantly demonstrates that when HRPTEC cultures are correctly polarized, form tight junctions, and concentrate OCT2 strictly on the basolateral membrane, cisplatin only induces toxicity when the basolateral membrane is exposed and at clinically relevant total-plasma concentrations (Himmelstein et al., 1981; Ikeda et al., 1998; Petrillo et al., 2019). Although the toxicity data presented in the current manuscript support OCT2-mediated cisplatin transport, future intracellular accumulation and transcellular transport studies using cisplatin as substrate may provide further insights into actual handling of this nephrotoxicant by the proximal tubule-on-a-chip. Cisplatin toxicity has previously been evaluated in a few chip-based models. Jang et al. (2013) showed that cisplatin exposed basolaterally induced toxicity in their 2D chip–based model, but the concentration used (100 μM) extends beyond the therapeutic concentration, and cellular cisplatin exposure was not evaluated (Himmelstein et al., 1981; Jang et al., 2013). In other studies, both compartments were used simultaneously, which prohibited any evaluation of the impact of epithelial polarization on cisplatin sensitivity (Suter-Dick et al., 2018; Vormann et al., 2018). In contrast to the current study, single-channel Nortis proximal tubule-on-a-chips were used to show that apical cisplatin exposure (1 μM) increased concentrations of Kidney Injury Molecule-1 in the supernatant, whereas LDH levels (reflecting cytotoxicity) were not affected (Sakolish et al., 2018; Maass et al., 2019). Although we can only speculate about the reason for the discrepancy compared with the current study, it may be explained by differences in exposure times and endpoints used, assays, cell source, and media components. An earlier study employing Lilly Laboratories Cell-Porcine Kidney 1 cells cultured on porous membrane inserts showed that basolateral treatment with cisplatin (300 μM) induced a higher degree of cytotoxicity compared with apical treatment, thus confirming the current findings, although the applied concentration was not regarded as clinically relevant, and localization of OCT2 was not investigated (Okuda et al., 1999a).

In contrast to the cisplatin parent compound, proximal tubule uptake of its metabolites is suggested to be mediated through alternative mechanisms (Townsend et al., 2009). Extrarenal glutathione conjugation generates water-soluble molecules capable of being filtered by the glomerulus, therefore mainly exposing the apical membrane of proximal tubule cells. Interestingly, inhibition of γ-glutamyl transpeptidase or cysteine s-conjugate β-lyase, which are vital enzymes in the conjugation pathway, or shifting the equilibrium toward oxidized glutathione can both reduce proximal tubule toxicity in mice, indicating that cisplatin-glutathione contributes to nephrotoxicity even when exposure is predominantly apical (Townsend and Hanigan, 2002; Jenderny et al., 2010). Extrarenal metabolite formation is not incorporated in the proximal tubule-on-a-chip described in the current study. However, it could be extended with a liver-on-a-chip compartment, making it suitable to study the contribution of metabolites to drug-induced nephrotoxicity, as shown earlier for ifosfamide and aristolochic acid (Choucha-Snouber et al., 2013; Chang et al., 2017).

Cisplatin efflux from the proximal tubule is mainly mediated by MATE1 (Yonezawa et al., 2006; Nakamura et al., 2010; Li et al., 2013).

The current study showed significantly increased gene expression of MATE1 and MATE2-k in chip-cultured HRPTECs compared with regular 2D cultures, which suggests a more physiologically relevant phenotype. However, immunofluorescence did not succeed in detecting specific staining of MATE1 or MATE2-k in the proximal tubule-on-a-chip (unpublished data), which was most likely because of poor specificity of the primary antibodies, thus requiring extended optimization. Therefore, localization of these transporters remains to be elucidated in future studies. Treating HPRTECs with bardoxolone methyl, an inducer of signaling by the nuclear factor erythroid 2–related factor 2 pathway, increases MATE1 gene expression and reduces cisplatin sensitivity (Atilano-Roque et al., 2016). Interestingly, nuclear factor erythroid 2–related factor 2 has also been shown to regulate MATE2-K in response to flow in proximal tubule cells (Fukuda et al., 2017), sparking speculation that Nrf signaling might explain upregulation of MATE gene expression observed in the current study.

Transepithelial transport activity is indicative of a polarized epithelial phenotype, as was previously shown for organic anions (Weber et al., 2016; Jansen et al., 2019; van der Made et al., 2019). The current study did not demonstrate a statistically significant inhibition of 4-di-1-ASP transepithelial transport using cimetidine and therefore concerted activity of OCT2 and MATE1/2-k. However, the observed trend in inhibition is in line with the findings by Stahl et al. (2020), who demonstrated transcellular transport of cation drug metformin in a proximal tubule-on-a-chip using the same chip platform, although a different tissue donor was employed. Differences in methods might explain this discrepancy because radioactively labeled metformin was used as cation substrate combined with inhibitor imipramine, and this substrate and inhibitor combination reflects a different inhibition potential. In addition, increased sensitivity of detection due to radioactive labeling compared with the fluorescent methods used in the current study potentially allows detection of inhibition across a wider range of substrate concentration (Stahl et al., 2020). In turn, variations in substrate transfer might reflect chip-to-chip differences in barrier integrity, increasing the diffusion component of substrate transfer across the epithelial tube and highlighting that advanced chip-based culture models remain technically challenging. MATE-mediated transport is driven by a concentration gradient of H^+ over the brush border membrane (Tsuda et al., 2007; Sato et al., 2008; König et al., 2011). It has been shown that evaluation of cisplatin transport by MATE1 in vitro requires artificially acidifying the cytoplasm and reversing the naturally occurring H^+ gradient and direction of MATE1-mediated transport (Nakamura et al., 2010). Therefore, transepithelial transport activity and MATE-mediated efflux of cisplatin in chip-cultured HRPTECs may be investigated in future studies by increasing the acidity of the luminal chip channel, providing a more physiologically relevant driving force. In addition, genetic knockdown or knockout approaches would be a suitable future strategy to provide more direct evidence of organic cation transporter– and MATE-mediated transport function in the currently developed proximal tubule-on-a-chip.

The current study found significantly increased gene expression of *LRP2* coding for the megalin endocytosis receptor in chip-cultured HRPECs compared with regular 2D HRPTEC cultures. Megalin is expressed on the apical brush border of proximal tubule cells and is responsible for reabsorption of low-molecular-weight proteins and albumin from the glomerular filtrate (Nielsen et al., 2016). Increased uptake of megalin substrate bovine serum albumin has been described in response to changes in fluid flow (Ferrell et al., 2012, 2018; Jang et al., 2013; Raghavan et al., 2014). More recently, endocytosis activity has also been implicated in the uptake of antisense oligonucleotides into the proximal tubule epithelium (Janssen et al., 2019). Therefore, future studies may investigate whether the proximal tubule model developed here is suited to study antisense oligonucleotide–induced renal adverse effects or the effects of fluid flow on receptor-mediated endocytosis.

In conclusion, the current study presented the first kidney proximal tubule-on-a-chip in which a nephrotoxic drug has been exposed through both the clinically relevant and nonrelevant compartments to demonstrate the contribution of epithelial polarization and membrane localization of drug influx mechanisms in achieving drug sensitivity at clinically relevant concentrations. Therefore, the developed in vitro model displays increased physiologic relevance compared with single-compartment models and could be applied in the future to improve preclinical prediction of drug-induced kidney toxicity and eventually reduce kidney-related adverse effects of candidate drugs in the clinic.

Acknowledgments

The authors would like to thank Pedro Pinto and Simone Stahl for practical training and extended discussions on the experimental setup. The authors thank Magnus Söderberg for discussions on research design. The authors thank Glen Hawthorne for quantification of the cisplatin perfusion samples and Sam Peel for providing imaging trays. The authors thank Otto Magnusson for contributing to the gene expression analysis. The authors offer special thanks to Marianna Stamou for expert help with imaging.

Authorship Contributions

Participated in research design: Nieskens, Kelly, Sjögren.
Conducted experiments: Nieskens.
Performed data analysis: Nieskens, Sjögren.
Wrote or contributed to the writing of the manuscript: Nieskens, Persson, Kelly, Sjögren.

References

Atilano-Roque A, Aleksunes LM, and Joy MS (2016) Bardoxolone methyl modulates efflux transporter and detoxifying enzyme expression in cisplatin-induced kidney cell injury. *Toxicol Lett* **259**:52–59.
Biermann J, Lang D, Gorboulev V, Koepsell H, Sindic A, Schröter R, Zvirbliene A, Pavenstädt H, Schlatter E, and Ciarimboli G (2006) Characterization of regulatory mechanisms and states of human organic cation transporter 2. *Am J Physiol Cell Physiol* **290**:C1521–C1531.
Brown CD, Sayer R, Windass AS, Haslam IS, De Broe ME, D'Haese PC, and Verhulst A (2008) Characterisation of human tubular cell monolayers as a model of proximal tubular xenobiotic handling. *Toxicol Appl Pharmacol* **233**:428–438.
Budiman T, Bamberg E, Koepsell H, and Nagel G (2000) Mechanism of electrogenic cation transport by the cloned organic cation transporter 2 from rat. *J Biol Chem* **275**: 29413–29420.
Chang SY, Weber EJ, Sidorenko VS, Chapron A, Yeung CK, Gao C, Mao Q, Shen D, Wang J, Rosenquist TA, et al. (2017) Human liver-kidney model elucidates the mechanisms of aristolochic acid nephrotoxicity. *JCI Insight* **2**:e95978.
Choucha-Snouber L, Aninat C, Grsicom L, Madalinski G, Brochot C, Poleni PE, Razan F, Guillouzo CG, Legallais C, Corlu A, et al. (2013) Investigation of ifosfamide nephrotoxicity induced in a liver-kidney co-culture biochip. *Biotechnol Bioeng* **110**:597–608.
Ciarimboli G, Deuster D, Knief A, Sperling M, Holtkamp M, Edemir B, Pavenstädt H, Lanvers-Kaminsky C, am Zehnhoff-Dinnesen A, Schinkel AH, et al. (2010) Organic cation transporter 2 mediates cisplatin-induced oto- and nephrotoxicity and is a target for protective interventions. *Am J Pathol* **176**:1169–1180.
Ciarimboli G, Ludwig T, Lang D, Pavenstädt H, Koepsell H, Piechota HJ, Haier J, Jaehde U, Zisowsky J, and Schlatter E (2005) Cisplatin nephrotoxicity is critically mediated via the human organic cation transporter 2. *Am J Pathol* **167**:1477–1484.
Ferrell N, Cheng J, Miao S, Roy S, and Fissell WH (2018) Orbital shear stress regulates differentiation and barrier function of primary renal tubular epithelial cells. *ASAIO J* **64**:766–772.
Ferrell N, Ricci KB, Groszek J, Marmerstein JT, and Fissell WH (2012) Albumin handling by renal tubular epithelial cells in a microfluidic bioreactor. *Biotechnol Bioeng* **109**:797–803.
Filipski KK, Loos WJ, Verweij J, and Sparreboom A (2008) Interaction of Cisplatin with the human organic cation transporter 2. *Clin Cancer Res* **14**:3875–3880.
Fukuda Y, Kaishima M, Ohnishi T, Tohyama K, Chisaki I, Nakayama Y, Ogasawara-Shimizu M, and Kawamata Y (2017) Fluid shear stress stimulates MATE2-K expression via Nrf2 pathway activation. *Biochem Biophys Res Commun* **484**:358–364.
Hartmann JT, Kollmannsberger C, Kanz L, and Bokemeyer C (1999) Platinum organ toxicity and possible prevention in patients with testicular cancer. *Int J Cancer* **83**:866–869.
Himmelstein KJ, Patton TF, Belt RJ, Taylor S, Repta AJ, and Sternson LA (1981) Clinical kinetics on intact cisplatin and some related species. *Clin Pharmacol Ther* **29**:658–664.
Ikeda K, Terashima M, Kawamura H, Takiyama I, Koeda K, Takagane A, Sato N, Ishida K, Iwaya T, Maesawa C, et al. (1998) Pharmacokinetics of cisplatin in combined cisplatin and 5-fluorouracil therapy: a comparative study of three different schedules of cisplatin administration. *Jpn J Clin Oncol* **28**:168–175.
Ito K, Suzuki H, Horie T, and Sugiyama Y (2005) Apical/basolateral surface expression of drug transporters and its role in vectorial drug transport. *Pharm Res* **22**:1559–1577.
Jang KJ, Mehr AP, Hamilton GA, McPartlin LA, Chung S, Suh KY, and Ingber DE (2013) Human kidney proximal tubule-on-a-chip for drug transport and nephrotoxicity assessment. *Integr Biol (Camb)* **5**:1119–1129.

Jansen J, De Napoli IE, Fedecostante M, Schophuizen CM, Chevtchik NV, Wilmer MJ, van Asbeck AH, Croes HJ, Pertijs JC, Wetzels JF, et al. (2015) Human proximal tubule epithelial cells cultured on hollow fibers: living membranes that actively transport organic cations. *Sci Rep* **5**:16702.

Jansen J, Jansen K, Neven E, Poesen R, Othman A, van Mil A, Sluijter J, Sastre Torano J, Zaal EA, Berkers CR, et al. (2019) Remote sensing and signaling in kidney proximal tubules stimulates gut microbiome-derived organic anion secretion. *Proc Natl Acad Sci U S A* **116**:16105–16110.

Janssen MJ, Nieskens TTG, Steevels TAM, Caetano-Pinto P, den Braanker D, Mulder M, Ponstein Y, Jones S, Masereeuw R, den Besten C, et al. (2019) Therapy with 2′-O-Me phosphorothioate antisense oligonucleotides causes reversible proteinuria by inhibiting renal protein reabsorption. *Mol Ther Nucleic Acids* **18**:298–307.

Jenderny S, Lin H, Garrett T, Tew KD, and Townsend DM (2010) Protective effects of a glutathione disulfide mimetic (NOV-002) against cisplatin induced kidney toxicity. *Biomed Pharmacother* **64**:73–76.

Katsuda H, Yamashita M, Katsura H, Yu J, Waki Y, Nagata N, Sai Y, and Miyamoto K (2010) Protecting cisplatin-induced nephrotoxicity with cimetidine does not affect antitumor activity. *Biol Pharm Bull* **33**:1867–1871.

König J, Müller F, and Fromm MF (2013) Transporters and drug-drug interactions: important determinants of drug disposition and effects. *Pharmacol Rev* **65**:944–966.

König J, Zolk O, Singer K, Hoffmann C, and Fromm MF (2011) Double-transfected MDCK cells expressing human OCT1/MATE1 or OCT2/MATE1: determinants of uptake and transcellular translocation of organic cations. *Br J Pharmacol* **163**:546–555.

Lash LH, Lee CA, Wilker C, and Shah V (2018) Transporter-dependent cytotoxicity of antiviral drugs in primary cultures of human proximal tubular cells. *Toxicology* **404–405**:10–24.

Lash LH, Putt DA, and Cai H (2006) Membrane transport function in primary cultures of human proximal tubular cells. *Toxicology* **228**:200–218.

Lash LH, Putt DA, and Cai H (2008) Drug metabolism enzyme expression and activity in primary cultures of human proximal tubular cells. *Toxicology* **244**:56–65.

Li Q, Guo D, Dong Z, Zhang W, Zhang L, Huang SM, Polli JE, and Shu Y (2013) Ondansetron can enhance cisplatin-induced nephrotoxicity via inhibition of multiple toxin and extrusion proteins (MATEs). *Toxicol Appl Pharmacol* **273**:100–109.

Maass C, Sorensen NB, Himmelfarb J, Kelly EJ, Stokes CL, and Cirit M (2019) Translational assessment of drug-induced proximal tubule injury using a kidney microphysiological system. *CPT Pharmacometrics Syst Pharmacol* **8**:316–325.

Nakamura T, Yonezawa A, Hashimoto S, Katsura T, and Inui K (2010) Disruption of multidrug and toxin extrusion MATE1 potentiates cisplatin-induced nephrotoxicity. *Biochem Pharmacol* **80**:1762–1767.

Nielsen R, Christensen EI, and Birn H (2016) Megalin and cubilin in proximal tubule protein reabsorption: from experimental models to human disease. *Kidney Int* **89**:58–67.

Nieskens TTG and Sjögren AK (2019) Emerging in vitro systems to screen and predict drug-induced kidney toxicity. *Semin Nephrol* **39**:215–226.

Nigam SK, Wu W, Bush KT, Hoenig MP, Blantz RC, and Bhatnagar V (2015) Handling of drugs, metabolites, and uremic toxins by kidney proximal tubule drug transporters. *Clin J Am Soc Nephrol* **10**:2039–2049.

Okuda M, Tsuda K, Masaki K, Hashimoto Y, and Inui K (1999a) Cisplatin-induced toxicity in LLC-PK1 kidney epithelial cells: role of basolateral membrane transport. *Toxicol Lett* **106**: 229–235.

Okuda M, Urakami Y, Saito H, and Inui K (1999b) Molecular mechanisms of organic cation transport in OCT2-expressing Xenopus oocytes. *Biochim Biophys Acta* **1417**:224–231.

Pabla N, Murphy RF, Liu K, and Dong Z (2009) The copper transporter Ctr1 contributes to cisplatin uptake by renal tubular cells during cisplatin nephrotoxicity. *Am J Physiol Renal Physiol* **296**:F505–F511.

Petrillo M, Zucchetti M, Cianci S, Morosi L, Ronsini C, Colombo A, D'Incalci M, Scambia G, and Fagotti A (2019) Pharmacokinetics of cisplatin during open and minimally-invasive secondary cytoreductive surgery plus HIPEC in women with platinum-sensitive recurrent ovarian cancer: a prospective study. *J Gynecol Oncol* **30**:e59.

Raghavan V, Rbaibi Y, Pastor-Soler NM, Carattino MD, and Weisz OA (2014) Shear stress-dependent regulation of apical endocytosis in renal proximal tubule cells mediated by primary cilia. *Proc Natl Acad Sci USA* **111**:8506–8511.

Sakolish C, Weber EJ, Kelly EJ, Himmelfarb J, Mouneimne R, Grimm FA, House JS, Wade T, Han A, Chiu WA, et al. (2018) Technology transfer of the microphysiological systems: a case study of the human proximal tubule tissue chip. *Sci Rep* **8**:14882.

Sato T, Masuda S, Yonezawa A, Tanihara Y, Katsura T, and Inui K (2008) Transcellular transport of organic cations in double-transfected MDCK cells expressing human organic cation transporters hOCT1/hMATE1 and hOCT2/hMATE1. *Biochem Pharmacol* **76**:894–903.

Schmidt EK, Antonin KH, Flesch G, and Racine-Poon A (1998) An interaction study with cimetidine and the new angiotensin II antagonist valsartan. *Eur J Clin Pharmacol* **53**:451–458.

Stahl S, Nordell P, Nieskens T, Fenner KS, and Caetano-Pinto P (2020) P245 - Investigation of renal drug secretion in a kidney-on-a-chip model. *Drug Metab Pharmacokinet* **35**:S97.

Stoops EH and Caplan MJ (2014) Trafficking to the apical and basolateral membranes in polarized epithelial cells. *J Am Soc Nephrol* **25**:1375–1386.

Suter-Dick L, Mauch L, Ramp D, Caj M, Vormann MK, Hutter S, Lanz HL, Vriend J, Masereeuw R, and Wilmer MJ (2018) Combining extracellular miRNA determination with microfluidic 3D cell cultures for the assessment of nephrotoxicity: a proof of concept study. *AAPS J* **20**:86.

Townsend DM and Hanigan MH (2002) Inhibition of gamma-glutamyl transpeptidase or cysteine S-conjugate beta-lyase activity blocks the nephrotoxicity of cisplatin in mice. *J Pharmacol Exp Ther* **300**:142–148.

Townsend DM, Tew KD, He L, King JB, and Hanigan MH (2009) Role of glutathione S-transferase Pi in cisplatin-induced nephrotoxicity. *Biomed Pharmacother* **63**:79–85.

Tsuda M, Terada T, Asaka J, Ueba M, Katsura T, and Inui K (2007) Oppositely directed H+ gradient functions as a driving force of rat H+/organic cation antiporter MATE1. *Am J Physiol Renal Physiol* **292**:F593–F598.

van der Made TK, Fedecostante M, Scotcher D, Rostami-Hodjegan A, Sastre Toraño J, Middel I, Koster AS, Gerritsen KG, Jankowski V, Jankowski J, et al. (2019) Quantitative translation of microfluidic transporter in vitro data to in vivo reveals impaired albumin-facilitated indoxyl sulfate secretion in chronic kidney disease. *Mol Pharm* **16**:4551–4562.

Vedula EM, Alonso JL, Arnaout MA, and Charest JL (2017) A microfluidic renal proximal tubule with active reabsorptive function. *PLoS One* **12**:e0184330.

Vormann MK, Gijzen L, Hutter S, Boot L, Nicolas A, van den Heuvel A, Vriend J, Ng CP, Nieskens TTG, van Duinen V, et al. (2018) Nephrotoxicity and kidney transport assessment on 3D perfused proximal tubules. *AAPS J* **20**:90.

Vriend J, Nieskens TTG, Vormann MK, van den Berge BT, van den Heuvel A, Russel FGM, Suter-Dick L, Lanz HL, Vulto P, Masereeuw R, et al. (2018) Screening of drug-transporter interactions in a 3D microfluidic renal proximal tubule on a chip. *AAPS J* **20**:87.

Weber EJ, Chapron A, Chapron BD, Voellinger JL, Lidberg KA, Yeung CK, Wang Z, Yamaura Y, Hailey DW, Neumann T, et al. (2016) Development of a microphysiological model of human kidney proximal tubule function. *Kidney Int* **90**:627–637.

Weber EJ, Lidberg KA, Wang L, Bammler TK, MacDonald JW, Li MJ, Redhair M, Atkins WM, Tran C, Hines KM, et al. (2018) Human kidney on a chip assessment of polymyxin antibiotic nephrotoxicity. *JCI Insight* **3**:e123673.

Wittwer MB, Zur AA, Khuri N, Kido Y, Kosaka A, Zhang X, Morrissey KM, Sali A, Huang Y, and Giacomini KM (2013) Discovery of potent, selective multidrug and toxin extrusion transporter 1 (MATE1, SLC47A1) inhibitors through prescription drug profiling and computational modeling. *J Med Chem* **56**:781–795.

Yonezawa A, Masuda S, Nishihara K, Yano I, Katsura T, and Inui K (2005) Association between tubular toxicity of cisplatin and expression of organic cation transporter rOCT2 (Slc22a2) in the rat. *Biochem Pharmacol* **70**:1823–1831.

Yonezawa A, Masuda S, Yokoo S, Katsura T, and Inui K (2006) Cisplatin and oxaliplatin, but not carboplatin and nedaplatin, are substrates for human organic cation transporters (SLC22A1-3 and multidrug and toxin extrusion family). *J Pharmacol Exp Ther* **319**:879–886.

Address correspondence to: Anna-Karin Sjögren, AstraZeneca R&D Mölndal, Pepparedsleden 1, 43150 Mölndal, Sweden. E-mail: anna-karin.sjogren@astrazeneca.com

DMD-AR-2020-000098

A human kidney proximal tubule-on-a-chip replicates cell polarization-dependent cisplatin toxicity

Tom T.G. Nieskens, Mikael Persson, Edward J. Kelly and Anna-Karin Sjögren

Drug Metabolism and Disposition

Supplemental Materials

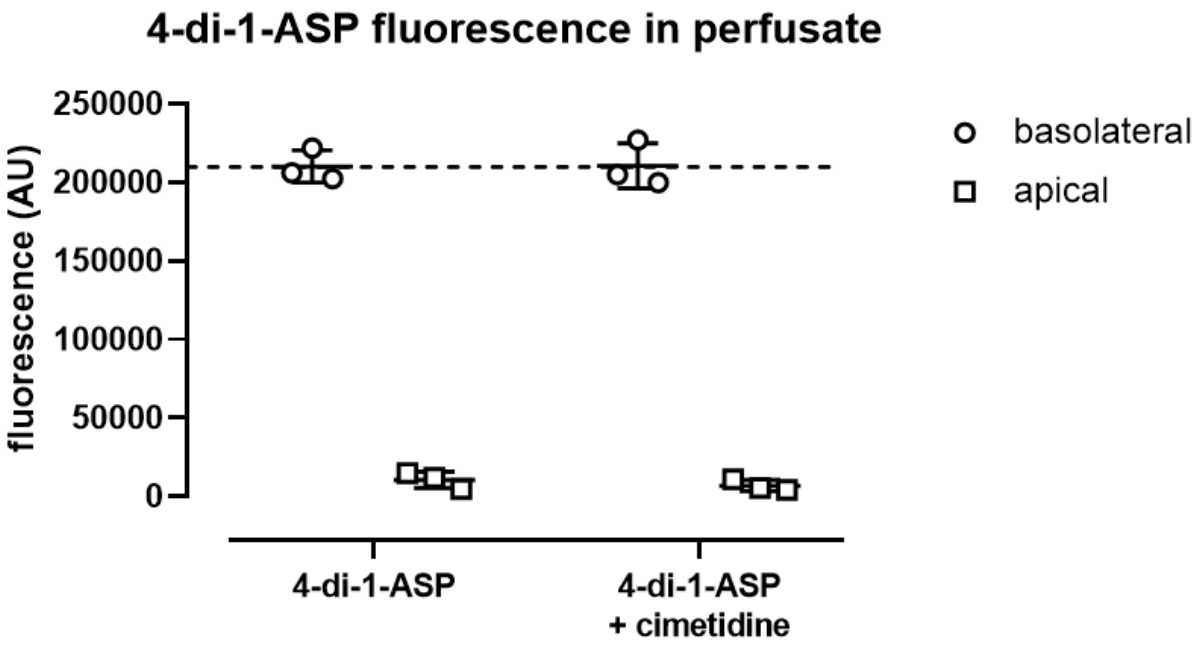

Figure S1: Fluorescent organic cation 4-di-1-ASP transepithelial transport assay in the proximal tubule-on-a-chip. Fluorescent cation 4-di-1-ASP (100 µM) was perfused at 2 µl/min into the basolateral compartment of the proximal tubule-on-a-chip, with or without OCT2 inhibitor cimetidine (1 mM), while buffer was perfused into the apical compartment. Fluorescence signal intensity of accumulative perfusate samples obtained from the basolateral and apical compartment for 14 h, initiated 6 h after perfusion was started. The basolateral fluorescence signal reflects the perfused concentration of 4-di-1-ASP (indicated by the dotted line), while the apical fluorescence signal is reduced as it reflects HRPTEC epithelial barrier integrity and transepithelial transport capacity.

DMD-AR-2020-000098

A human kidney proximal tubule-on-a-chip replicates cell polarization-dependent cisplatin toxicity

Tom T.G. Nieskens, Mikael Persson, Edward J. Kelly and Anna-Karin Sjögren

Drug Metabolism and Disposition

Supplemental Materials

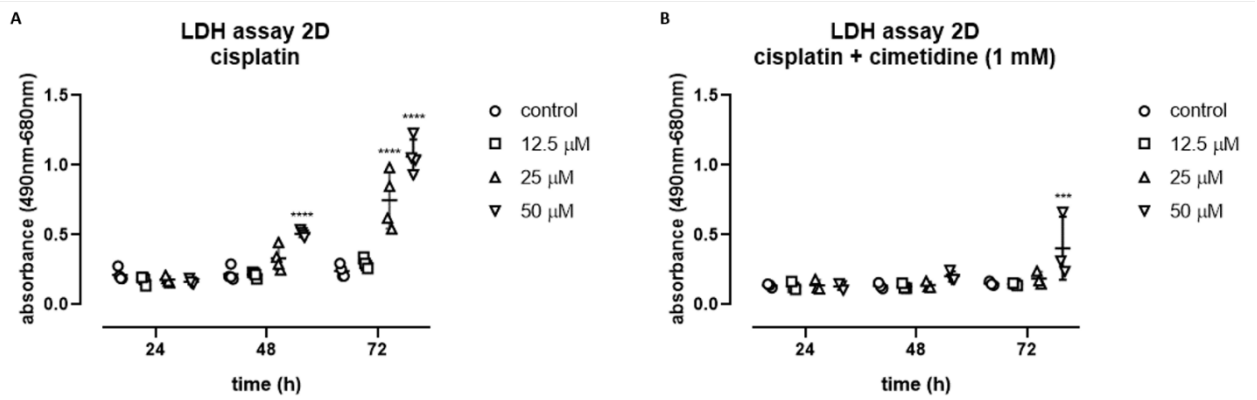

Figure S2: Cisplatin-induced toxicity and attenuation by cimetidine in regular 2D HRPTEC cultures. Time and concentration dependent increase of LDH activity in the supernatant of 2D HRPTEC cultures following exposure to cisplatin (12.5; 25 and 50 µM) for 24, 48 and 72 h in (A) absence or (B) presence of OCT2 inhibitor cimetidine (1 mM) (mean±S.D., cisplatin concentration compared to time-matched control by two-way ANOVA with Dunnett's multiple comparisons test, n=4 (A) and n=3 (B) with all biological replicates set in advance, performed with 2 experimental replicates, 9 comparisons in total, ***P<0.001; ****P<0.0001 (multiplicity adjusted P values)).

DMD-AR-2020-000098

A human kidney proximal tubule-on-a-chip replicates cell polarization-dependent cisplatin toxicity

Tom T.G. Nieskens, Mikael Persson, Edward J. Kelly and Anna-Karin Sjögren

Drug Metabolism and Disposition

Supplemental Materials

Table S1: Primary and secondary antibodies and compounds for immunofluorescent staining

target	primary	secondary	channel	exposure
ZO-1	ZO1-1A12 Mouse 1:50 Invitrogen 33-9100 Lot TE268259 and UB280528	Goat anti-mouse Alexa Fluor 488 1:100 Life Technologies A21121 Lot 2083196	FITC	250 ms[a] 2000 ms[b]
Lotus Lectin	Biotinylated Lotus lectin Tetragonolobus purpureus 1:300 Vector Labs B1325 Lot ZC2428	Streptavidin conjugate Alexa Fluor 647 1:100 Life Technologies S21374 Lot 1941447	Cy5	150 ms[a] 1500 ms[b]
F-actin	Phalloidin conjugate Alexa Fluor 647 1:100 Life Technologies A22287 Lot 1941485		Cy5	50 ms[a] 2000 ms[b]
Nucleus	Hoechst 33342 1:1000 Life Technologies H3570 Lot 1932420		DAPI	50 ms[a] 500 ms[b]
OCT2	SLC22A2 Rabbit 1:50 Sigma HPA008567 B114258	Goat anti-rabbit Alexa Fluor 594 1:100 Life Technologies A11037 Lot 1777945	Cy5	500 ms[a]
Primary cilia	Acetylated alpha-tubulin Mouse monoclonal 1:10,000 Sigma T7451 Lot 059M4812V	Goat anti-Mouse Alexa Fluor 647 1:500 Life Technologies A21242 Lot 1930629	Cy5	50 ms[a] 5000 ms[b]

[a]widefield imaging, [b]spinning disk confocal imaging

DMD-AR-2020-000098

A human kidney proximal tubule-on-a-chip replicates cell polarization-dependent cisplatin toxicity

Tom T.G. Nieskens, Mikael Persson, Edward J. Kelly and Anna-Karin Sjögren

Drug Metabolism and Disposition

Supplemental Materials

Table S2: Gene-specific primer probe sets for gene expression analysis (Applied Biosystems)

Gene name	Product code
GAPDH	Hs99999905_m1
HPRT1	Hs99999909_m1
ABCB1	Hs00184500_m1
ABCC4	Hs00988721_m1
ABCG2	Hs01053790_m1
SLC5A2	Hs00894642_m1
SLC22A1	Hs00427552_m1
SLC22A2	Hs01010726_m1
SLC22A4	Hs00268200_m1
SLC22A5	Hs00929869_m1
SLC22A6	Hs00537914_m1
SLC22A8	Hs00188599_m1
SLC31A1	Hs00741015_m1
SLC47A1	Hs00217320_m1
SLC47A2	Hs00945652_m1
SLCO4C1	Hs00698884_m1
LRP2	Hs00189742_m1
CUBN	Hs00153607_m1
AQP1	Hs01028916_m1
TJP1	Hs01551861_m1
GGT1	Hs00980756_m1